J Nanostruct 11(2): 323-332, Spring 2021

RESEARCH PAPER

Optoelectronic Performances of Au and CuO Nanoparticles Incorporated Organic Photovoltaic Devices

Aruna P. Wanninayake

Department of Physics and Electronics, University of Kelaniya, Kelaniya, Sri Lanka

ARTICLE INFO

Article History:
Received 05 January 2021
Accepted 27 March 2021
Published 01 April 2021

Keywords:
Au NPs
CuO NPs
P3HT
Plasmonic effect
Polymer Solar Cells

ABSTRACT

Direct conversion of Solar energy to electrical energy using nanostructured organic/inorganic hybrid semiconductors is one of the best solutions for today's energy crisis. In particular, researchers are turning their attention to the incorporation of metal or transition metal oxide nanoparticles (NPs) into the active layer of polymer solar cells (PSCs) to increase the power conversion efficiency. The design approaches for incorporation of metal NPs such as gold (Au) is based on localized plasmonic resonance effect (LSPR) which can be used to enhance the optical absorption in photovoltaic devices. Meanwhile, the transition metal oxide NPs such as Cuprous oxide (CuO) NPs in the active layer play a key role as light-harvesting centers, charge particle hopping centers, and surface morphology developer enabling a considerable reduction in the physical thickness of photovoltaic absorber layers. In this study, Au and CuO NPs are incorporated into poly(3-hexylthiophene)(P3HT)/ [6:6]-phenyl-C61-butyric acid (PCBM) active layer to enhance the power conversion efficiency (PCE) of the PSCs.. The influence of the Au and CuO NPs in the P3HT/PCBM was investigated using UV–Vis spectroscopy, scanning electron microscopy and atomic force microscopy. Electrical characteristics of the devices were analyzed from J –V characteristics and external quantum efficiency measurement to observe the performance of the P3HT:PCBM PSCs. The addition of Au and CuO NPs increased the power conversion efficiency by 48.7% compared to the reference cell. The short circuit current(J_{sc}) of the optimum cell was measured at 7.218 mA/cm^2.~~compared to 5.338 mA/cm^2 in the reference cells.~~ Also, the external quantum efficiency(EQE) increased from 45% to 68.5%, showing 52.2% enhancement. The Au and CuO-NPs improved the charge collection at the anode, which results in higher short circuit current and fill factor.

How to cite this article
Wanninayake A.P. Optoelectronic Performances of Au and CuO Nanoparticles Incorporated Organic Photovoltaic Devices. J Nanostruct, 2021; 11(2):323-332. DOI: 10.22052/JNS.2021.02.013

INTRODUCTION

Bulk heterojunction (BHJ) polymer solar cells (PSCs) which are based on conjugated polymer donor and fullerene derivative acceptor materials have attracted much attention due to the efficient charge transfer from conjugated polymers to fullerene derivatives. Compared to inorganic solar cells, Polymer solar cells (PSCs) usually have one important hindrance for the efficiency improvement with insufficient light absorption due to the thin active layer which is restricted by the short exciton diffusion length and low carrier mobility[1-3]. In recent years, tremendous effort has been taken to develop the light absorption of

* *Corresponding Author Email: wannina@kln.ac.lk*

the polymer solar cells and increase the power conversion efficiencies (PCE) of single junction cells and the PCE has exceeded 14% of the single junction solar cells. This development is a result of the tuning of active layer materials with light absorption counterparts, development of the surface morphology of the thin films, reducing the series and shunt resistance of the devices etc. The Regioregularpoly(3-hexylthiophene) (P3HT) and [6,6]-phenyl C61-bu-tyric acid methyl ester (PCBM) blend is one of the common and promising materials for achieving high PCE because of the high self-organizing ability, high hole mobility, and broad range absorption in the red region of the electromagnetic spectrum. However, more efficient Sun energy harvesting requires the compounds to absorb strongly in the visible region of the spectrum [4-5].

Illuminated metallic nanoparticles (NPs) such as Au and other metallic nanostructures can be used to enhance the light absorption of the polymer thin films due to the localized surface plasmon resonance (LSPR) effect which enables to a remarkable enhancement of local electromagnetic fields [6,7]. The LSPR of metallic NPs is referred to as the collective oscillation of electrons residing on the metallic NPs are excited by the incident light photons at the resonant frequency [8]. The LSPR excitation of the metallic NPs results the improved electromagnetic fields, light absorption and scattering due to their physical and elemental parameters, which leads enhanced device performances. Considering the strong LSPR effect of the metallic NPs such as Ag and Au, many researchers have been widely investigated them for difference technological applications including photovoltaic device fabrications [9,10]. Brown et al [11] have shown that the metallic nanostructures in the active layer can scatter the incident photons through a long propagation path resulting a higher light absorption and photocurrent generation of PSCs. Lu et al [12] reported 20% enhancement of power conversion efficiency of Au and Ag incorporated PSCs due to the LSPR effect.

On the other hand, NPs of transition metal oxides such as copper oxide nanoparticles (CuO NPs) have gained special attention due to the low cost, non-toxic, and high optical absorption capabilities. CuO is a p-type semiconductor with a direct band gap energy of 1.5eV which is close to the ideal energy gap of 1.4eV for fabricating the high optical absorbing solar cells [13–16]. In the previously reported work by the author [17-19] has shown that incorporation of the CuO NPs in the active layer increased the power conversion efficiency (PCE) of the solar cells by 40.6%.

Many previous researches have been done on tuning the polymer solar cells with inorganic nanoparticles (NPs). The inorganic NPs of various sizes and configurations have been integrated into organic solar cell architecture in order to fine tune and enhance the morphology, electronic and optical absorption of respective PSCs. As a result, significant enhancements in the power conversion has been obtained. Depending on the position in the PSC architecture, incorporation of NPs can be categorized into three main groups which are: (i) photoactive or hole transport layers, (ii) buffer layers, and (iii) between different interfaces [20]. Table 1 summarizes the reported electrical parameters of such studies indicating the respective efficiency improvements.

However, there is no reported work for incorporating both Au NPs and CuO NPs in the active layer of PSCs. Therefore, this study will be extended to investigate the effect of the CuO NPs together with Au NPs in the P3HT/PCBM (poly (3-hexylthiophene)/ [6, 6]-phenyl-C70-butyric acid

Table 1. The reported electrical parameters of polymer solar cells

NPs	Size (nm)	J_{sc}(A/cm^2)	V_{oc}(V)	FF	PCE	Ref.
ZnO	<100	11.9	0.57	49	3.39	[21]
ZnO	<15	12.2	0.55	52	3.50	[22]
ZnO	<35	9.3	0.67	61	3.84	[23]
ZnO	50	10.4	0.58	53	3.20	[24]
Au	18	8.9	0.63	62	3.50	[25]
Au	30-40	10.2	0.59	69	4.19	[26]
Au	1.5-20	9.7	0.60	63	3.71	[27]
Ag	20	7.03	0.61	48	2.06	[28]
Ag	60	8.07	0.58	58	2.75	[29]
TiO_2	60	10.29	0.60	60	3.69	[30]
TiO_2	20-40	2.75	0.44	35	0.42	[31]
Ag-TiO_2	<100	9.5	0.64	65	3.96	[32]

methyl ester) active layer of the polymer solar cell devices. Also, the effect of the Au and CuO NPs on P3HT/ PCBM devices will be demonstrated through the optoelectronic and nano-scale morphology aspects and reveal their influences on PCE of the Solar cells. The optoelectronic and morphological parameters are comparatively studied by UV absorption, SEM, EQE, AFM and solar simulation.

MATERIALS AND METHODS

Poly(3-hexylthiophene) (P3HT) (Rieke Metals), phenyl-C70butyric acid methyl ester (PC70BM) (SES Research), Nanoparticles of gold (Au) (15 nm diameter) and Nanoparticles of CuO (10-30nm diameter) (nanocs.com), Glass substrates measuring 24 x 80 x 1.2 mm (12 Ω/cm^2) with an Indium Tin Oxide (ITO) conductive layer of 25-100 nm (nanocs.com) and Aluminium coils with a diameter of 0.15 mm (Ted-Pella, Inc.) were used as received. poly(3,4ethylenedioxythiophene)-poly(styrenesulfonate) (PEDOT/PSS) mixed in distilled water was obtained from Sigma Aldrich and it was mixed with an equal amount of distilled water. All processing and characterization work of the PSC devices were conducted under the same experimental conditions.

Device Fabrication

The conductive glass substrates were ultrasonically cleaned with ammonium hydroxide, hydrogen peroxide, distilled water, methyl alcohol, and isopropyl alcohol; successively. The fabrication of polymer based solar cells containing Au-NPs was carried out in a N_2 filled glove box. The P3HT-PC70BM blend was obtained by diluting equal amounts of regioregular P3HT and PC70BM (10 mg each) with 2 ml of chlorobenzene (C_6H_5Cl) and mixing for 14 hours at 50°C. The next step is the incorporation of Au-NPs (15 nm diameter) and CuO-NPs into the blend by dispersing NPs in 2 ml of chlorobenzene and adding it to the P3HT/PCBM blend in weights leading to be the final weight ratios (P3HT/PCBM/AuNPs/CuO-NPs) of 10:10:0:0; 10:10:0.05:0; 10:10:0:0.6; and 10:10:0.05:0.6 mg, respectively.

The solar cell devices were spun coated in a glove box with N_2 atmosphere. A 40 nm-thick PEDOT/PSS layer, which serves as a thin hole-transport layer, was spun coated at a rotational velocity of 4000 rpm, followed by heating at 120°C for 20 minutes in the air. When the temperature of the samples reached the ambient temperature, the blends with P3HT: PC70BM: Au-NPs: CuO

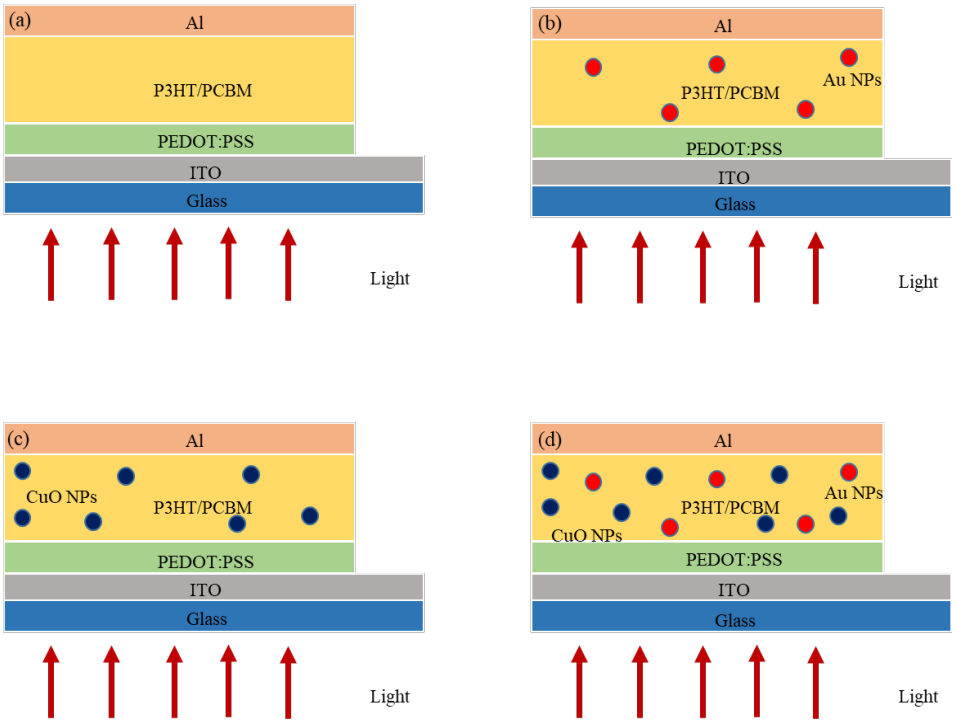

Fig. 1. Schematic illustration of polymer solar cells: (a) Reference solar cell without nanoparticles, (b) Au NPs incorporated solar cells, (c) CuO NPs incorporated cells, (d) Au and CuO NPs incorporated solar cells

NPs solution was spun coated for two minutes at 1000 rpm. The active layers measured 120 nm in average thickness and 0.12 cm^2 in surface area. A schematic illustration of the layered structure of the fabricated devices is shown in Fig. 1.

Characterization

Current density–voltage (J-V) characterization was carried out for all PSCs using a UV solar simulator with an AM 1.5G filter and a lamp intensity of 100 mW/cm^2. A source meter (Keithley 2400) was used to obtain the J-V measurements. Device parameters; such as short circuit current (J_{sc}), open circuit voltage (V_{oc}), fill factor (FF) and power conversion efficiency (PCE) were recorded under ambient conditions. A quantum efficiency measurement kit (Newport-425) embedded in the solar cell simulator was used to obtain EQE values. A PerkinElmer LAMBDA 650 spectrophotometer was used to obtain the optical properties of cells.

An Agilent 5420 atomic force microscope(AFM) was used to analyze the surface morphology. The Pico Image Basics and Gwyddion software were utilized to determine the root mean square roughness (σ_{rms}) of the surface under ACAFM non-contact mode with set point 1.60, I-gain of 10, and scanned area of 2x2µm. The layer structures of the fabricated solar cells were analyzed using a scanning electron microscope with an energy dispersive x-ray detector (FEG-SEM Hitachi S-4800).

RESULTS AND DISCUSSION

PSC devices based on four different concentrations of Au and CuO NPs were fabricated and tested under simulated 100 mW cm^{-2} AM1.5G illumination. Table 2 indicates the photovoltaic parameters, such as J_{sc}, V_{oc}, fill factor (FF) (equation 1), and PCE (equation 2), of all the fabricated devices.

$$FF = \frac{J_m V_m}{J_{sc} V_{oc}} \quad (1)$$

$$PCE = \eta = \frac{J_{sc} V_{oc}\, FF}{P_{in}} \quad (2)$$

Where, P_{in} is the input power.

Summarized data demonstrates that the V_{oc} remained nearly the same for all four types of devices. The V_{oc} is directly related to the energy difference between the LUMOs of donor and acceptor materials which should be larger than 0.3 eV for efficient excitonic dissociation [33, 34]. But, the V_{oc} of organic solar cells is restricted by the difference between the HOMO of the donor and the LUMO of the acceptor. However, the above results imply that the positions of the HOMO of the donor and the LUMO of the acceptor was not altered by Au or CuO NPs in the active layer. In spite of the V_{oc} trend, it is clear that the J_{sc} increased from 5.338 mA/cm^2 to 6.228 mA/cm^2 by adding Au NPs in the active layer. The J_{sc} was further increased from6.228 mA/cm^2 to 6.829 mA/cm^2 after adding CuO NPs into the P3HT/PCBM active layer. However, the highest J_{sc} value of 7.218 mA/cm^2 was exhibited by the PSCs which are contained both Au and CuO NPs in the active layer. The FF values enhanced from 61% to 66%. However, the FF value remained unchanged at 66% without depending on the type of the NPs. The FF explains the combination of the series resistance (R_s) and shunt resistance (R_{sh}) of the device. R_s represents the sum of contact resistance on the front/back surfaces and the ohmic resistances. Shunt resistance is mainly due to the imperfections on the device surface [35]. The Au NPs and CuO NPs did not show a significant influence on the resistance of the device. These improved J_{sc} and FF influenced PCE and it was enhanced from 2.114%

Table 2. Performance parameters of hybrid solar cells

CuO NPs (mg)	Au NPs (mg)	J_{sc} (mA/cm^2)	V_{oc} (V)	FF (%)	PCE (%)
0	0.00	5.338	0.65	61	2.114
0	0.05	6.228	0.65	66	2.672
0.6	0.00	6.829	0.66	66	2.975
0.6	0.05	7.218	0.66	66	3.144

to 3.144% by incorporating Au and CuO NPs in the same P3HT/PCBM active layer. This increased in PCE translates to a 48.7% total enhancement of the PCE in comparison to the reference cells. Fig. 2 shows J-V characteristics curves of ITO/PEDOT: PSS/ P3HT /PCBM/Al solar cells with different concentrations of Au NPs and CuO NPs in the P3HT/PCBM active layer.

The J_{sc} of the solar cell device has a linear relationship with the EQE which is theoretically indicated as equation 3.

$$J_{sc} = \frac{q}{\hbar C}\int_{\lambda_{min}}^{\lambda_{max}} EQE\ P_{in}(\lambda)\ \lambda\ d\lambda \qquad (3)$$

where q is the value of the charge, ħ is the reduced Planck constant, C and λ are the velocity and the wavelength of the light respectively.

The EQE is a ratio between the incident photons on the solar cell from the input light and the generated free charge carriers by the solar cell. The EQE can be modified as internal quantum efficiency (IQE) neglecting reflectance and transmittance of the incident photons to consider only the portion of the absorbed light by the active region. In the organic semiconductor based solar cells, EQE can be determined by five major factors which are composed of inherent efficiency components [19] which can be shown in equation 4.

$$EQE = \eta_A \cdot \eta_{diff} \cdot \eta_{diss} \cdot \eta_{tr} \cdot \eta_{cc} \qquad (4)$$

Here, η_A, η_{diff}, η_{diss}, η_{tr} and η_{cc} are represented the light absorption efficiency, the excitonic diffusion efficiency, the excitonic dissociation efficiency, the charge transport efficiency, and the electrons-holes collection efficiency respectively.

The shape of the EQE can be used to understand the material properties of the device and it is strongly correlated to the junction thickness and blend composition of the active layer. Furthermore, the shape of the EQE explains the mechanisms for free carrier generation in the active layer region. To confirm the accuracy of the J-V measurements, the EQE spectrum of the devices which were fabricated using four different concentrations of Au and CuO NPs was measured. The EQE curves are shown in Fig. 3. Corresponding EQE spectra for solar cells are improved from 45% to 68.5%. These all the devices exhibit efficient photoconversion in the range of 400–750 nm. To obtain such higher EQE values, it is requisite to accomplish enhanced and efficient light absorption, exciton diffusion,

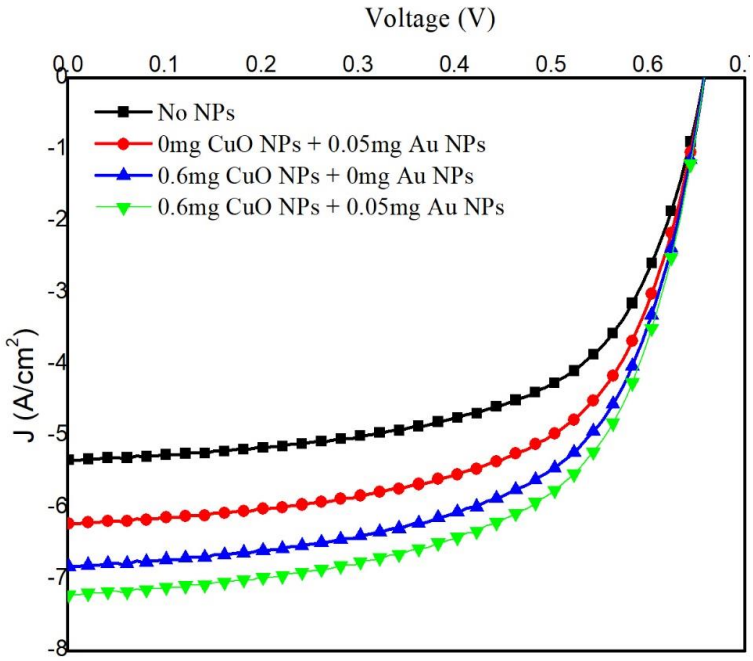

Fig. 2. J-V characteristics of P3HT/PCBM/Au-CuO NPs hybrid polymer solar cells

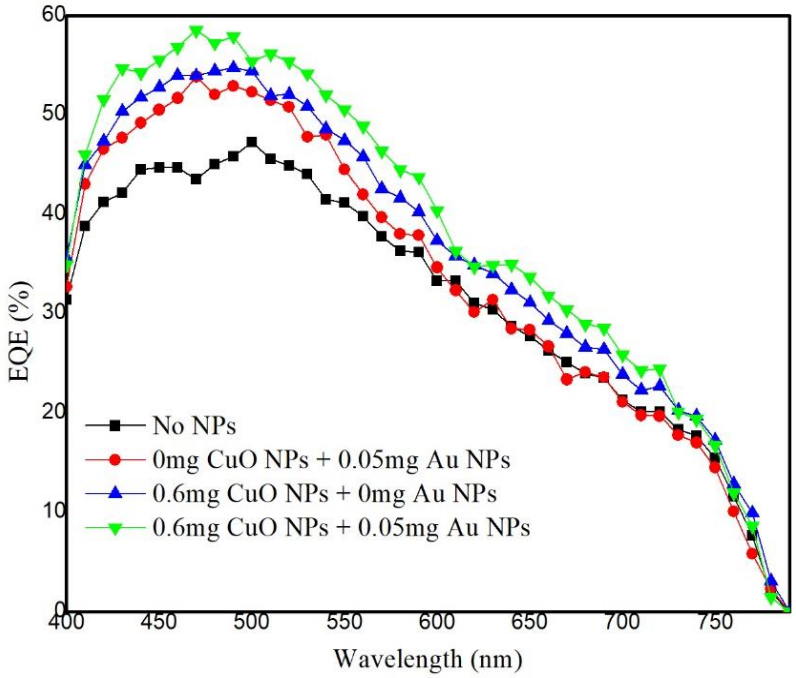

Fig. 3. EQE of the hybrid solar cells with various concentrations of Au and CuO NPs in the P3HT/PCBM active layer

charge carrier separation, and charge collection at the electrodes. Therefore, this improved EQE conduct to better elucidate improved Jsc relevant to the enhanced free carrier generation.

The metal nanostructures exhibit one of the most important properties is plasmonic behavior which is the collective oscillation of free electrons in the metal structure. Other properties of metal nanostructures such as reflection and transmission occur when the frequency of the incident light is below the plasma frequency and above the plasma frequency respectively. Frequently, the range of the plasma frequency of metals is in the ultraviolet domain, which leads to plasma reflective in the visible range. The plasmonic energy of such structures can be written as equations 5 and 6.

$$E_0 = \hbar\omega_0 \tag{5}$$

$$\omega_0 = \hbar\sqrt{\frac{ne^2}{m\varepsilon_0}} \tag{6}$$

where n is the electron density, e is the electron charge, m is the electron mass, is the permittivity of the free space, is the Planck constant, and is the plasmon frequency.

On the other hand, surface plasmons related to a metallic nanoparticle can be considered as localized surface plasmons (LSPs). When the light shines on the metallic nanoparticles, the electrons associated with the surface of the NPs are subjected to collective oscillate called LSPs as shown in Fig. 4. In addition, the Mie solution to Maxwell's equations for the spherical nanoparticles explains the scattering and absorption phenomena of the incident light. The correlation of the absorption cross-section (and the scattering cross-section (σ_{sc}) of the metal nanoparticles to the extinction cross-section (can be shown in equation 7 [36, 37].

$$\sigma_{ext} = \sigma_{ab} + \sigma_{sc} \tag{7}$$

This plasmonic behavior of the Au NPs is a crucial factor of increasing the light absorption in the fabricated polymer solar cells in this study. Photo-absorption and carrier generating ability of a polymer thin film are represented by the photon absorption (η_A) efficiency as shown in equation 4. Also, the light absorption of a semiconductor thin film is controlled by the energy band structure, absorption coefficient, and the thickness of the photoactive layer [38, 39]. On the other hand, the CuO NPs can be considered as the P3HT tuning materials due to their suitable energy band

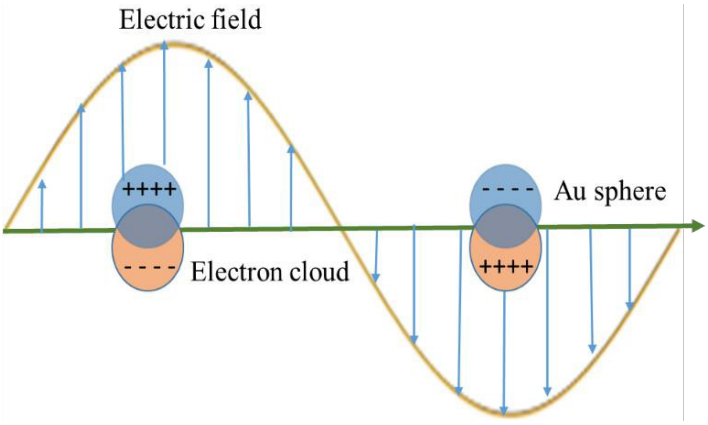

Fig. 4. localized surface plasmon resonance (LSPR), resulting from the collective oscillations of delocalized electrons in response to an external electric field

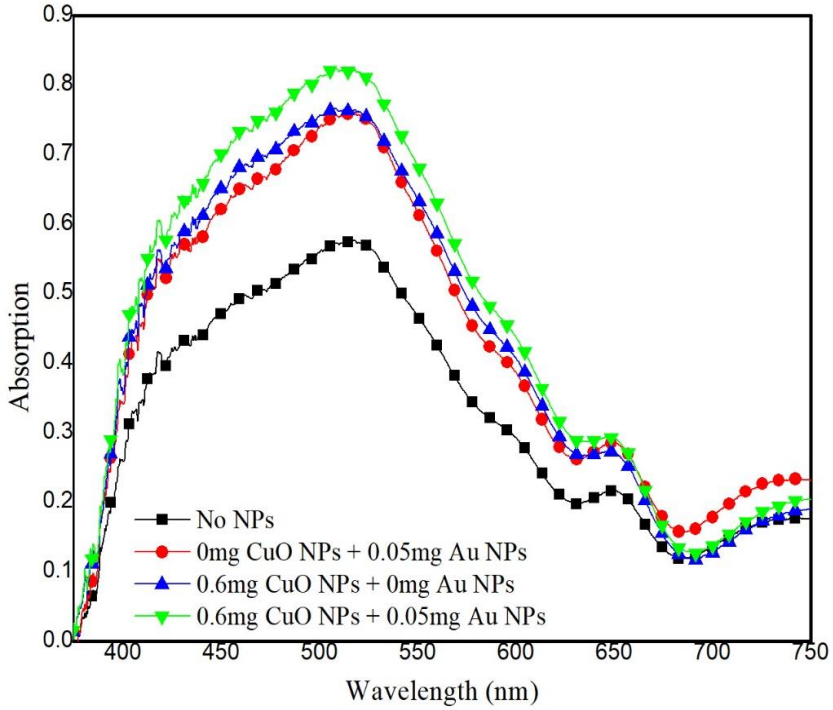

Fig. 5. Optical absorption spectra of the hybrid solar cells

structure and photo-electrons donor properties. Therefore, CuO NPs may increase the exciton generation and dissociation process in the PSCs. Also, CuO NPs play a role being charge hopping centers for charge carriers enabling high charge mobility within the structure. N.R. Dhineshbabu et al [14] reported that the CuO NPs have shown high optical absorbance at UV region, and then it decreases exponentially in the visible region near the IR region.

So the CuONPs are very high absorptive at the UV region and they are more convenient for the fabrication of the solar cells. Also, the CuO thin film has a high optical absorption coefficient which is conducive to increase the probability of direct transition occurrence. On the other hand, the CuO nanoparticles consist of small nanocrystalline clusters with different orientation of the single crystal diffraction pattern and, the CuO nanoparticles encourage the formation of P3HT crystallites reducing the charge carrier diffusion length. Therefore, these

CuO NPs clusters and crystallized P3HT enhance the charge carrier hopping process minimizing the charge recombination. These inherent composites ~~inherent~~ properties of the Au and CuO NPs were used to enhance the light absorption of the P3HT/PCBM solar cells. The UV-vis absorption This reduced bandgap is encouraged the smooth transition of the free electrons from the donor material to the acceptor material. The UV-vis absorption, EQE, and J_{sc} measurements were significantly increased showing the same trend. Therefore, it can be identified that the plasmonic effect (LSPR) of Au NPs and absorption properties of CuO NPs play a significant role in enhanced PCE of the solar cell devices.

The AFM images of the P3HT/PCBM with different concentrations of Au and CuO NPs dispersed films were obtained to understand the surface morphology of the active layer as shown in fig. 6. Significantly different morphologies were observed for these four types of devices in their AFM images. The root-mean-square roughness (R_{rms}) is linearly correlated with the interfacial surface area between the active layer and PEDOT: PSS hole collection layer or Al cathode. The increase of the interfacial surface area leads to the efficient dissociation of excitons into holes and electrons. The P3HT/PCBM layer showed a relatively smooth surface with root-mean-square roughness (R_{rms}) value of 0.10 nm. It was noticed that the R_{rms} value of the P3HT/PCBM layer was increased with increasing the concentration of the NPs in the P3HT/PCBM blend. The R_{rms} of the device with 0.05 Au NPs was 0.81 nm. However, it was exhibited 0.32 nm in the samples containing 0.6 mg of CuO NPs. Furthermore, the R_{rms} value was enhanced up to 0.91nm of the P3HT/PCBM layers incorporated with both CuO and Au NPs as shown in table 3.

This increased surface roughness contributes to enlarge the interfacial contact area between the PEDOT: PSS and P3HT/PCBM-CuO/Au NPs

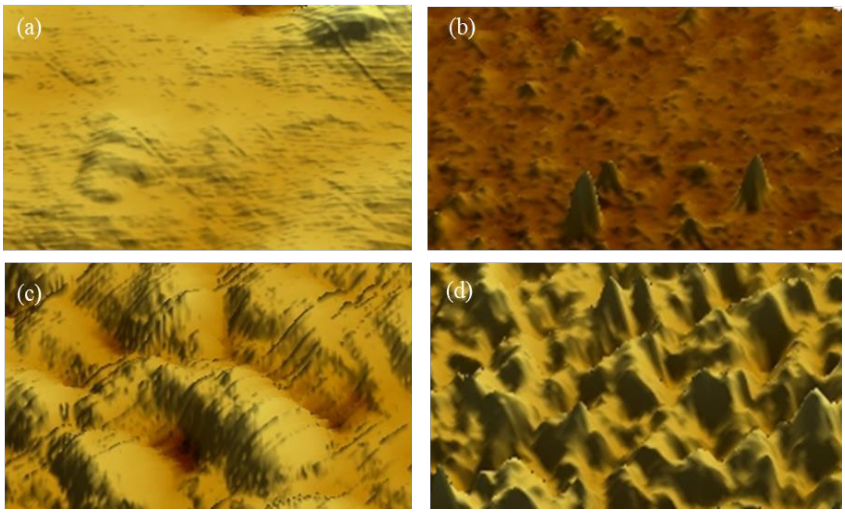

Fig. 6. AFM images for P3HT/PCBM layers with (a) no NPs, (b) 0mg CuO NPs + 0.05mg Au NPs, (c) 0.6mg CuO NPs + 0mg Au NPs, (d) 0.6mg CuO NPs + 0.05mg Au NPs

Table 3. Rrms values of the PSCs with different concentration of Au/CuO NPs

Sample	CuO NPs (mg)	Au NPs (mg)	R_{rms} (nm)
(a)	0.00	0.00	0.10
(b)	0.00	0.05	0.81
(c)	0.60	0.00	0.32
(d)	0.60	0.05	0.91

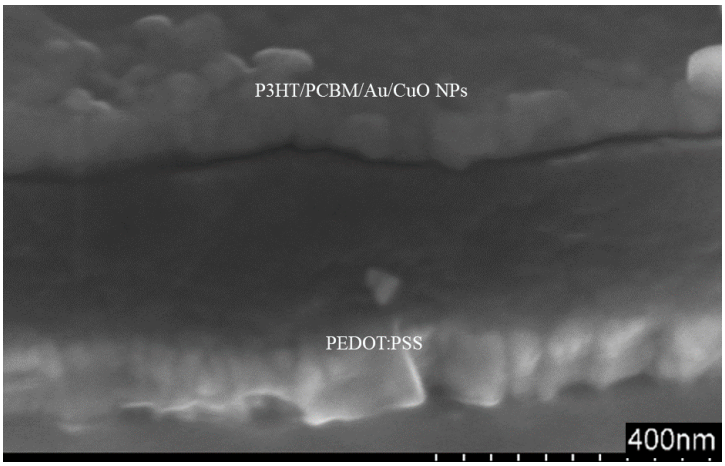

Fig. 7. SEM images of the P3HT/PCBM/Au/CuO NPs hybrid polymer solar cell

layers, allowing high efficient hole collection at the anode and hence improve the J_{sc} and shape of the FF. Also, this increased surface roughness of the cells with Au and CuO NPs is evidence of adequate space for P3HT crystallites to form in the active layer structure. Higher P3HT crystals discourage the fully amorphous PCBM molecules to dissolve in the P3HT domain, thus promoting the aggregation of PCBM, which will contribute to better P3HT/PCBM phase separation. The SEM images of the hybrid structure of the fabricated PEDOT: PSS/ P3HT: PCBM/Au-CuO NPs/device are shown in the Fig. 7. The Au and CuO-NPs added the P3HT/PCBM active layer was approximately in the range of 100-160nm thickness. It is helpful to eliminate the charge recombination losses in the devices. The thickness of the PEDOT: PSS hole transport layer was estimated as 40nm.

CONCLUSION

In this study, Au and CuO-NPs were added to the P3HT/PCBM layer of solar cells in order to increase the power conversion efficiency. The PCE increased from 2.114 to 3.144% in the cells containing 0.05 mg Au-NPs and 0.6mg CuO-NPs, which is equivalent to 48.7% improvement of efficiency. The higher performance is attributed to enhanced UV-vis absorption, EQE and J_{sc}. The optical absorption spectrum changed significantly after presence of Au-NPs in the P3HT/PCBM active layer due to the strong near field around Au-NPs. EQE of the solar cells increased due to the increased hole and electron polaron mobilities in cells with Au and CuO NPs. AFM analysis showed an increase in surface roughness of the P3HT/PCBM active layer with Au and CuO NPs, which is an indication of larger space to form the P3HT crystallites. Also, the FF was enhanced by adding these Au and CuO NPs in the cells, but it was a constant value with different concentrations of the NPs.

CONFLICT OF INTEREST

The authors declare that there are no conflicts of interest regarding the publication of this manuscript.

REFERENCES

1. Dang MT, Hirsch L, Wantz G. P3HT:PCBM, Best Seller in Polymer Photovoltaic Research. Advanced Materials. 2011;23(31):3597-602.
2. P. Wanninayake A, C. Church B, Abu-Zahra N. Effect of ZnO nanoparticles on the power conversion efficiency of organic photovoltaic devices synthesized with CuO nanoparticles. AIMS Materials Science. 2016;3(3):927-37.
3. Li G, Shrotriya V, Yao Y, Yang Y. Investigation of annealing effects and film thickness dependence of polymer solar cells based on poly(3-hexylthiophene). Journal of Applied Physics. 2005;98(4):043704.
4. Liu K, Bi Y, Qu S, Tan F, Chi D, Lu S, et al. Efficient hybrid plasmonic polymer solar cells with Ag nanoparticle decorated TiO2 nanorods embedded in the active layer. Nanoscale. 2014;6(11):6180.
5. Spyropoulos GD, Stylianakis MM, Stratakis E, Kymakis E. Organic bulk heterojunction photovoltaic devices with surfactant-free Au nanoparticles embedded in the active layer. Applied Physics Letters. 2012;100(21):213904.
6. Sepúlveda B, Angelomé PC, Lechuga LM, Liz-Marzán LM. LSPR-based nanobiosensors. Nano Today. 2009;4(3):244-51.
7. Bansal A, Sekhon JS, Verma SS. Scattering Efficiency and LSPR Tunability of Bimetallic Ag, Au, and Cu Nanoparticles. Plasmonics. 2013;9(1):143-50.
8. Liu D, Li L, You T. Superior catalytic performances of platinum nanoparticles loaded nitrogen-doped graphene toward methanol oxidation and hydrogen evolution reaction. Journal of Colloid and Interface Science. 2017;487:330-5.

9. Fu L, Li C, Li Y, Chen S, Long Y, Zeng R. Simultaneous determination of iodide and bromide using a novel LSPR fluorescent Ag nanocluster probe. Sensors and Actuators B: Chemical. 2017;240:315-21.
10. Reisdorffer F, Haas O, Le Rendu P, Nguyen TP. Co-solvent effects on the morphology of P3HT:PCBM thin films. Synthetic Metals. 2012;161(23-24):2544-8.
11. Brown MD, Suteewong T, Kumar RSS, D'Innocenzo V, Petrozza A, Lee MM, et al. Plasmonic Dye-Sensitized Solar Cells Using Core−Shell Metal−Insulator Nanoparticles. Nano Letters. 2011;11(2):438-45.
12. Lu L, Luo Z, Xu T, Yu L. Cooperative Plasmonic Effect of Ag and Au Nanoparticles on Enhancing Performance of Polymer Solar Cells. Nano Letters. 2012;13(1):59-64.
13. Sun B, Marx E, Greenham NC. Photovoltaic Devices Using Blends of Branched CdSe Nanoparticles and Conjugated Polymers. Nano Letters. 2003;3(7):961-3.
14. Dhineshbabu NR, Rajendran V, Nithyavathy N, Vetumperumal R. Study of structural and optical properties of cupric oxide nanoparticles. Applied Nanoscience. 2015;6(6):933-9.
15. Salim E, Bobbara SR, Oraby A, Nunzi JM. Copper oxide nanoparticle doped bulk-heterojunction photovoltaic devices. Synthetic Metals. 2019;252:21-8.
16. Saunders BR, Turner ML. Nanoparticle–polymer photovoltaic cells. Advances in Colloid and Interface Science. 2008;138(1):1-23.
17. Wanninayake AP, Gunashekar S, Li S, Church BC, Abu-Zahra N. CuO Nanoparticles Based Bulk Heterojunction Solar Cells: Investigations on Morphology and Performance. Journal of Solar Energy Engineering. 2015;137(3).
18. Wanninayake AP, Gunashekar S, Li S, Church BC, Abu-Zahra N. Effect of Thermal Annealing on the Power Conversion Efficiency of CuO-Bulk Heterojunction P3HT/ PC70BM Solar Cells. Journal of Sustainable Energy Engineering. 2015;3(2):107-26.
19. Wanninayake AP, Gunashekar S, Li S, Church BC, Abu-Zahra N. Performance enhancement of polymer solar cells using copper oxide nanoparticles. Semiconductor Science and Technology. 2015;30(6):064004.
20. Liang Z, Zhang Q, Jiang L, Cao G. ZnO cathode buffer layers for inverted polymer solar cells. Energy & Environmental Science. 2015;8(12):3442-76.
21. Oh SH, Heo SJ, Yang JS, Kim HJ. Effects of ZnO Nanoparticles on P3HT:PCBM Organic Solar Cells with DMF-Modulated PEDOT:PSS Buffer Layers. ACS Applied Materials & Interfaces. 2013;5(22):11530-4.
22.Zhu F, Chen X, Lu Z. Efficiency Enhancement of Inverted Polymer Solar Cells Using Ionic Liquid-functionalized Carbon Nanoparticles-modified ZnO as Electron Selective Layer. Nano-Micro Lett, 2014: 6(1): 24-29.
23. Gao HL, Zhang XW, Meng JH, Yin ZG, Zhang LQ, Wu JL, et al. Enhanced efficiency in polymer solar cells via hydrogen plasma treatment of ZnO electron transport layers. Journal of Materials Chemistry A. 2015;3(7):3719-25.
24. Sekine N, Chou C-H, Kwan WL, Yang Y. ZnO nano-ridge structure and its application in inverted polymer solar cell. Organic Electronics. 2009;10(8):1473-7.
25. Fung DDS, Qiao L, Choy WCH, Wang C, Sha WEI, Xie F, et al. Optical and electrical properties of efficiency enhanced polymer solar cells with Au nanoparticles in a PEDOT–PSS layer. Journal of Materials Chemistry. 2011;21(41):16349.
26.Chen F. C, Wu J. L, Lee C. L. Plasmonic-enhanced polymer photovoltaic devices incorporating solution- processable metal nanoparticles. Appl Phys Lett, 2009; 95: 013305.
27. Spyropoulos GD, Stylianakis MM, Stratakis E, Kymakis E. Organic bulk heterojunction photovoltaic devices with surfactant-free Au nanoparticles embedded in the active layer. Applied Physics Letters. 2012;100(21):213904.
28. Paci B, Spyropoulos GD, Generosi A, Bailo D, Albertini VR, Stratakis E, et al. Enhanced Structural Stability and Performance Durability of Bulk Heterojunction Photovoltaic Devices Incorporating Metallic Nanoparticles. Advanced Functional Materials. 2011;21(18):3573-82.
29. Yang J, You J, Chen C-C, Hsu W-C, Tan H-r, Zhang XW, et al. Plasmonic Polymer Tandem Solar Cell. ACS Nano. 2011;5(8):6210-7.
30. Hu X, Xiong J, Tang Y, Zhou C, Yang J. Interface modification of polymer solar cells using graphene oxide and TiO2 NPs. physica status solidi (a). 2014;212(3):585-90.
31. Kwong CY, Choy WCH, Djuri i AB, Chui PC, Cheng KW, Chan WK. Poly(3-hexylthiophene):TiO2nanocomposites for solar cell applications. Nanotechnology. 2004;15(9):1156-61.
32. Liu K, Bi Y, Qu S, Tan F, Chi D, Lu S, et al. Efficient hybrid plasmonic polymer solar cells with Ag nanoparticle decorated TiO2 nanorods embedded in the active layer. Nanoscale. 2014;6(11):6180.
33. Wang TL, Shieh YT, Yang CH, Ho TH, Chen CH. Photovoltaic properties and annealing effects of a low bandgap copolymer containing dithienothiophene and benzothiadiazole units. Express Polymer Letters. 2013;7(1):63-75.
34. Park MS, Kim FS. Synergistic Effects of Processing Additives and Thermal Annealing on Nanomorphology and Hole Mobility of Poly(3-hexylthiophene) Thin Films. Polymers (Basel). 2019;11(1):112.
35. Zhang Z, Miao J, Ding Z, Kan B, Lin B, Wan X, et al. Efficient and thermally stable organic solar cells based on small molecule donor and polymer acceptor. Nat Commun. 2019;10(1):3271-.
36. Uddin A, Yang X. Surface Plasmonic Effects on Organic Solar Cells. Journal of Nanoscience and Nanotechnology. 2014;14(2):1099-119.
37. Ferry VE, Sweatlock LA, Pacifici D, Atwater HA. Plasmonic Nanostructure Design for Efficient Light Coupling into Solar Cells. Nano Letters. 2008;8(12):4391-7.
38. Atwater HA, Polman A. Plasmonics for improved photovoltaic devices. Nature Materials. 2010;9(3):205-13.
39. Schuller JA, Barnard ES, Cai W, Jun YC, White JS, Brongersma ML. Plasmonics for extreme light concentration and manipulation. Nature Materials. 2010;9(3):193-204.
40. Kim K, Carroll DL. Roles of Au and Ag nanoparticles in efficiency enhancement of poly(3-octylthiophene)/C60 bulk heterojunction photovoltaic devices. Applied Physics Letters. 2005;87(20):203113.